DISCRETE-TIME DYNAMIC MODEL OF A MAGNETO-RHEOLOGICAL DAMPER FOR SEMI-ACTIVE CONTROL DESIGN

Claudio Crivellaro
Dana Structural Solutions Brazil
e-mail: claudio.crivellaro@dana.com

Decio Crisol Donha
State University of São Paulo (USP) – Escola Politécnica – DEM
e-mail: decdonha@usp.br

Abstract. *Semi-active control systems have been widely studied over the last 20 years. The range of applications includes automotive suspensions, seismic vibration mitigation, large bridges vibration control, knee prosthesis, among others. Semi-active actuators have a complex dynamics, and interaction between actuator and plant cannot be ignored in control design. This is specially true for magneto-rheological dampers, which are semi-active force actuators exhibiting a hysteretic behavior during velocity change of direction and where the force itself is dependent of the damper velocity. This work presents a new discrete-time dynamic model of magneto-rheological dampers, validated by experimental data.*

Keywords*: dynamic model, magneto-rheological, discrete-time, Non-linear, Bouc-Wen, damper.*

1. INTRODUCTION

In recent years, semi-active control devices have received significant attention because they offer the adaptability of active control devices without requiring the associated large power sources.

Magneto-rheological (MR) devices are semi-active control actuators that use MR fluids to produce controllable dampers, brakes or clutches. They potentially offer highly reliable operation and can be viewed as fail-safe since they become passive devices in case of control hardware malfunction.

Nowadays there have already been several commercial applications of this kind of semi-active actuator. For example, there are use of MR devices in prosthetic leg (Medical Product Manufacturing News, 2000), washing machine vibration control (Chrzan and Carlson, 2001), in building seismic response reduction (Dyke *et al.*, 1996), in rain-wind-induced cable vibration reduction in sprung bridges (Ni *et al.*, 2002), passenger car suspension control (Gilbert and Jackson, 2002), mountain bicycle suspension control (Breese and Gordaninejad, 2003), and others described in Carlson *et al.* (1999).

To use the semi-active actuator, several techniques of control design have been applied, as can be seen in works by Crivellaro (2003), Bodie and Hać (2000), and Hać *et al.* (1996). To develop control algorithms that take maximum advantage of the unique features of the MR damper, mathematical models must be developed so that the intrinsic nonlinear behavior of the damper could be adequately characterized.

Based on the work developed by Spencer *et al.* (1996) and on the need of digital applications of control, we propose an improved discrete model for a MR damper.

Using experimental data, the proposed model behavior was fitted to the real device behavior via Matlab™ Minimax optimization algorithm based on Sequential Quadratic Programming (SQP). The results show that the proposed model can effectively portray the behavior of typical magneto-rheological dampers and that it is adequate for control design application and analysis.

2. MAGNETO-RHEOLOGICAL DAMPER

A Magneto-Rheological (MR) damper is very similar to the traditional damper as shown in Spencer *et al.* (1996). The difference lies on the use of a magneto-rheological fluid, which typically consists of micron sized, magnetically polarizable particles dispersed in a carrier medium such as mineral or silicone oil (Bombard *et al.*, 2002). When a magnetic field is applied to the fluid, particle chains are formed, and the fluid becomes semi-solid, exhibiting plastic behavior, changing the flow properties of the fluid. Transitions to rheological equilibrium can be achieved in a few milliseconds, providing devices with high bandwidth. A MR damper could be build using a traditional damper body with magnetic valves able to act over the MR fluid property. The peak power required to fluid control is less than 30 watts, which could allow the damper to operate continuously for more then an hour on a small battery.

A schematic drawing of a MR damper is shown in Fig. 1. This schematic drawing emphasizes the magnetic choke, which generates a magnetic field to control the fluid rheological behavior; and the accumulator, which absorbs the volume variation due to the entrance of the rod inside the fluid camera. The accumulator in general consists of a bladder or an air camera with a movable piston pressurized at $2 \cdot 10^6$ Pa.

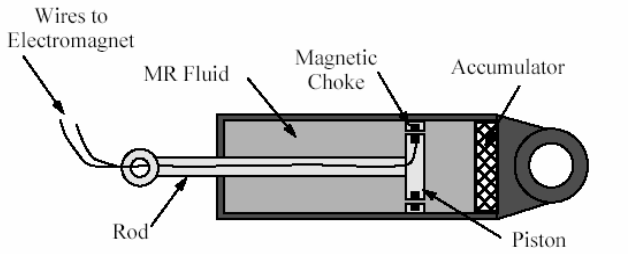

Figure 1. Schematic of MR damper.

Built in this way these dampers have the property of generating forces in the opposite sense of the movement of the piston, which come from two sources: the first is the same of the traditional dampers, corresponding to a viscous friction, which generates forces proportional to the speed of the piston. The second is related to the effect of the magneto-rheological fluid behavior within the piston under the adjustable magnetic field, which resultant force does not just depend on the speed, but also on the electric current (or indirectly of the electric tension) applied to the magnetic choke. In this case, the dependence of the speed is not linear as in the viscous friction, and it shows a kind of hysteretic behavior between force and velocity. This hysteretic behavior is intensified by the elastic effect of bushings at the joints of damper.

3. DISCRETE MODEL FORMULATION

The schematic diagram of the mechanical model proposed in this work is shown in the Fig. 2. In this picture, the variable x means the displacement of damper rod and F is the reaction force of damper rod under x displacement and $\dot{x}$ velocity. The parameters k_0 and c_0 are respectively the spring stiffness of the accumulator and the damping coefficient of the viscosity.

The variable ζ [1] is the evolutionary variable used to emulate a Bouc-Wen hysteretic model (Wen, 1976, *apud* Spencer *et al.*, 1996), which is a numerically tractable model and has been extensively used (Spencer *et al.*, 1996).

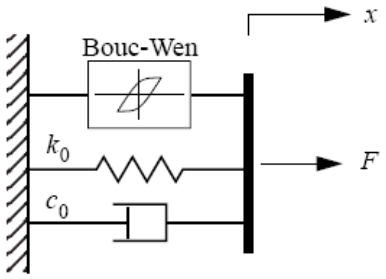

Figure 2. The MR Damper proposed model.

The original equations by Spencer *et al.* (1996) are reproduced below:

$$\dot{\zeta} = -\gamma \cdot |\dot{x}| \cdot \zeta \cdot |\zeta|^{n-1} - \beta \cdot \dot{x} \cdot |\zeta|^{n} + A \cdot \dot{x} \tag{1}$$

$$\dot{u} = -\eta \cdot (u - \nu) \tag{2}$$

$$F = c_0(u) \cdot \dot{x} + k_0 \cdot (x - x_0) + \alpha(u) \cdot \zeta \tag{3}$$

$$\alpha(u) = \alpha_a + \alpha_b \cdot u \tag{4}$$

$$c_0(u) = c_{0a} + c_{0b} \cdot u \tag{5}$$

[1] In the original work by Spencer *et al*. 1996, they used the letter "z" instead "ζ" to represent the Bouc-Wen evolutionary variable. Here we changed it to avoid confusion with the operator "z" in discrete z-transfer functions.

The model inputs are $x(t), \dot{x}(t)$ and $v(t)$, and the model output is $F(t)$, and there are eleven parameters: $n, \gamma, \beta, A, \eta, k_0, x_0, \alpha_a, \alpha_b, c_{0a}$ and c_{0b}. The control input is the variable v showed in Eq. (2), which unit is volt. There are only two state variables: $\zeta(t)$, which is the Bouc-Wen evolutionary variable, and $u(t)$, the variable proportional to the electrical current in the magnetic choke.

Adjusting the parameters of the model (in special γ, β and A), we can control the linearity in the unloading and the smoothness of transition from the pre-yield to the post-yield region. In addition, the accumulator force, f_0, can be directly incorporated into this model as an initial flexion x_0 of the linear spring k_0.

Although this continuous-time model is suitable to develop control algorithms for semi-active controllers, taking maximum advantage of the unique features of the MR damper, it is not appropriate to digital control application. Digital applications require discrete-time models, which could work with data sampled in a fixed rate. In addition, a discrete-time approach can be implemented in a micro-controller algorithm and used as model reference for more sophisticated control strategies, considering the dynamic behavior of the actuator.

The main goal of this work is to propose a new discrete-model for MR dampers. This model is obtained from an approximation of a continuous-time Bouc-Wen model by a discrete-time representation.

To get the discrete-model, the Eq. (1) is modified. The parameter n was fixed as 2, and the input variable $\dot{x}$ was defined as $v_x(t)$. This differential equation is then written as follows:

$$\dot{\zeta} = \frac{d\zeta}{dt} = -\gamma \cdot |v_x| \cdot \zeta \cdot |\zeta| - \beta \cdot v_x \cdot \zeta^2 + A \cdot v_x \tag{6}$$

A simple way of converting the differential equation to a difference equation is to approximate the derivative of the state by a difference. There are two simple choices, a *forward difference*, also called *Eulers's method*, that could be seen in Eq. (7), where h is the sample interval and the sampling instances are $t_k = kh$, where k is a integer positive number.

$$\frac{d\zeta(t)}{dt} \approx \frac{\zeta(t+h) - \zeta(t)}{h} = \frac{z-1}{h} \cdot \zeta(kh) \tag{7}$$

or a *backward difference*, as shown in Eq. (8).

$$\frac{d\zeta(t)}{dt} \approx \frac{\zeta(t) - \zeta(t-h)}{h} = \frac{1-z^{-1}}{h} \cdot \zeta(kh) \tag{8}$$

With the forward-difference approximation, a stable continuous-time system may be mapped into an unstable discrete-time system. When the backward-difference approximation is used, a stable continuous-time system will always give a stable discrete-time system.

Applying the backward-difference approximation on Eq.(6), we have:

$$\frac{\zeta(kh) - \zeta(kh-h)}{h} = -\gamma \cdot |v_x(kh)| \cdot \zeta(kh) \cdot |\zeta(kh)| - \beta \cdot v_x(kh) \cdot [\zeta(kh)]^2 + A \cdot v_x(kh) \tag{9}$$

$$\Rightarrow \frac{\zeta(k) - \zeta(k-1)}{h} = -\gamma \cdot |v_x(k)| \cdot \zeta(k) \cdot |\zeta(k)| - \beta \cdot v_x(k) \cdot [\zeta(k)]^2 + A \cdot v_x(k) \tag{10}$$

$$\Rightarrow \zeta(k) + \gamma \cdot h \cdot |v_x(k)| \cdot \zeta(k) \cdot |\zeta(k)| + \beta \cdot h \cdot v_x(k) \cdot [\zeta(k)]^2 = A \cdot h \cdot v_x(k) + \zeta(k-1) \tag{11}$$

The quadratic terms are eliminated as follows. One of the factors of multiplication was backward shifted by one time interval, as shown in Eq. (12):

$$\zeta(k) + \gamma \cdot h \cdot |v_x(k)| \cdot \zeta(k) \cdot |\zeta(k-1)| + \beta \cdot h \cdot v_x(k) \cdot \zeta(k) \cdot \zeta(k-1) = A \cdot h \cdot v_x(k) + \zeta(k-1) \tag{12}$$

The discrete-time form of Bouc-Wen model is given by:

$$\zeta(k) = \frac{A \cdot h \cdot v_x(k) + \zeta(k-1)}{1 + \gamma \cdot h \cdot |v_x(k)| \cdot |\zeta(k-1)| + \beta \cdot h \cdot v_x(k) \cdot \zeta(k-1)} \tag{13}$$

In the same way, the backward difference approximation could be applied to Eq. (2) given:

$$\frac{u(k)-u(k-1)}{h} = -\eta \cdot \left(u(k) - v(k)\right) \tag{14}$$

To improve the model flexibility and to compensate the lost degree of freedom in the Bouc-Wen model due to the discretization process, the parameters γ, β and A are now dependent of $u(k)$ via polynomial functions, and the order of polynomial functions of α and c_0 was augmented. In addition, a parameter ξ was included in Eq. (13). Therefore the new discrete-time model can be described by the following difference and polynomial equations:

$$u(k) = \frac{\eta \cdot h \cdot v(k) + u(k-1)}{1 + \eta \cdot h} \tag{15}$$

$$\gamma(u(k)) = \gamma_a + \gamma_b \cdot u(k) + \gamma_c \cdot u(k)^2 \tag{16}$$

$$\beta(u(k)) = \beta_a + \beta_b \cdot u(k) \tag{17}$$

$$A(u(k)) = A_a + A_b \cdot u(k) + A_c \cdot u(k)^2 \tag{18}$$

$$\zeta(k) = \frac{A(u(k)) \cdot h \cdot v_x(k) + \zeta(k-1)}{\xi + \gamma(u(k)) \cdot h \cdot \left|v_x(k)\right| \cdot \left|\zeta(k-1)\right| + \beta(u(k)) \cdot h \cdot v_x(k) \cdot \zeta(k-1)} \tag{19}$$

$$\alpha(u(k)) = \alpha_a + \alpha_b \cdot u(k) + \alpha_c \cdot u(k)^2 + \alpha_d \cdot u(k)^3 + \alpha_e \cdot u(k)^4 + \alpha_f \cdot u(k)^5 \tag{20}$$

$$c_0(u(k)) = c_{0a} + c_{0b} \cdot u(k) + c_{0c} \cdot u(k)^2 \tag{21}$$

$$F(k) = c_0(u(k)) \cdot v_x(k) + k_0 \cdot \left(x(k) - x_0\right) + \alpha(u(k)) \cdot \zeta(k) \tag{22}$$

The new discrete-time model has 21 parameters to be adjusted. The input variables are $x(k)$, $v_x(k)$ and $v(k)$, and the output is $F(k)$.

4. MR DAMPER PROTOTYPE

A MR Damper prototype was built following the design methodology proposed and presented in Crivellaro and Santos (2004). The design goal was to build a prototype of Ford Ranger frontal shock absorber. We have considered a monotube concept using an accumulator with movable embolus.

The fluid used in the prototype is a result of a research in the University UNIFEI in Itajubá, MG, in Brazil (Bombard, 2005).

Figures 3 and 4 show pictures of the prototype disassembled and assembled, respectively.

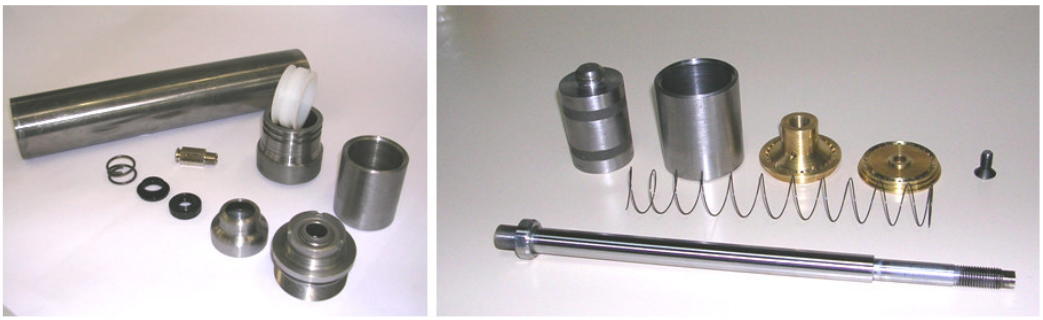

Figure 3 – MR damper prototype disassembled.

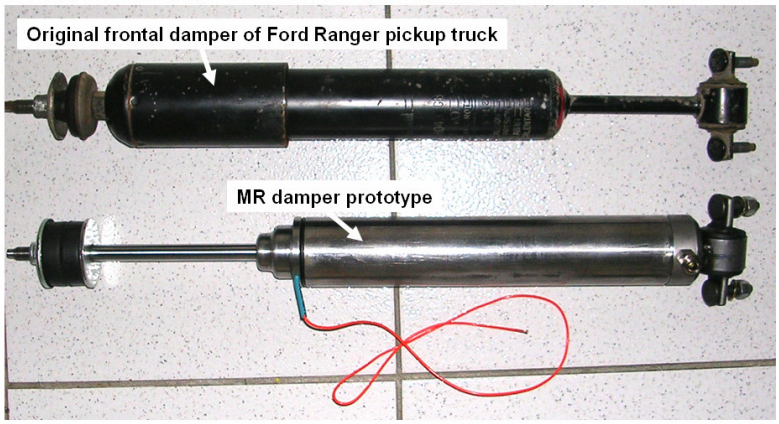

Figure 4 – MR damper prototype assembled.

5. EXPERIMENTAL STRUCTURE AND EQUIPMENTS

A load frame was designed and built to obtain the MR damper response data necessary for identification studies. The schematic diagram of this load frame with the signals path and equipments is shown in Fig. 5.

In this setup, a double-ended hydraulic actuator, manufactured by MTS, was employed to drive the damper. This actuator is endowed with a linear displacement measurement system, which was used to measure the displacement of the piston-rod of the MR damper. A MTS ±15kN load cell was included in series with the damper to measure the output force. The voltage control signal (from 0 to 10V) applied in the MR damper input is boosted by an electronic amplifier, which could supply until 3A at 10V.

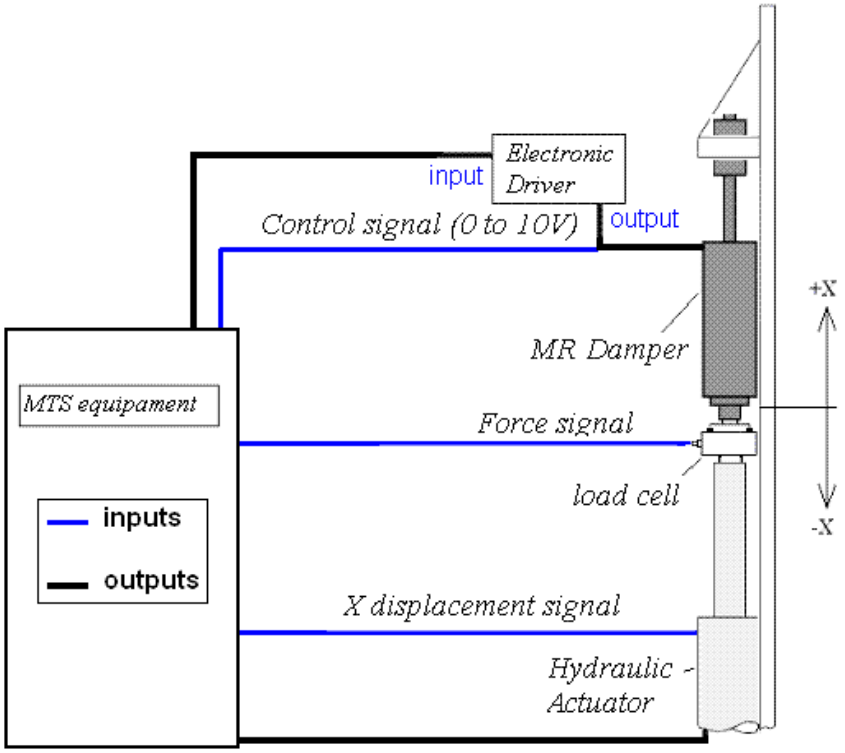

Figure 5 – Test Setup Schematic Diagram.

Three signals (force, piston-rod displacement, and MR damper control voltage) were sampled at 1024Hz rate by a MTS acquisition data unit.

Figure 6 shows the physical implementation of load frame used in MR damper tests.

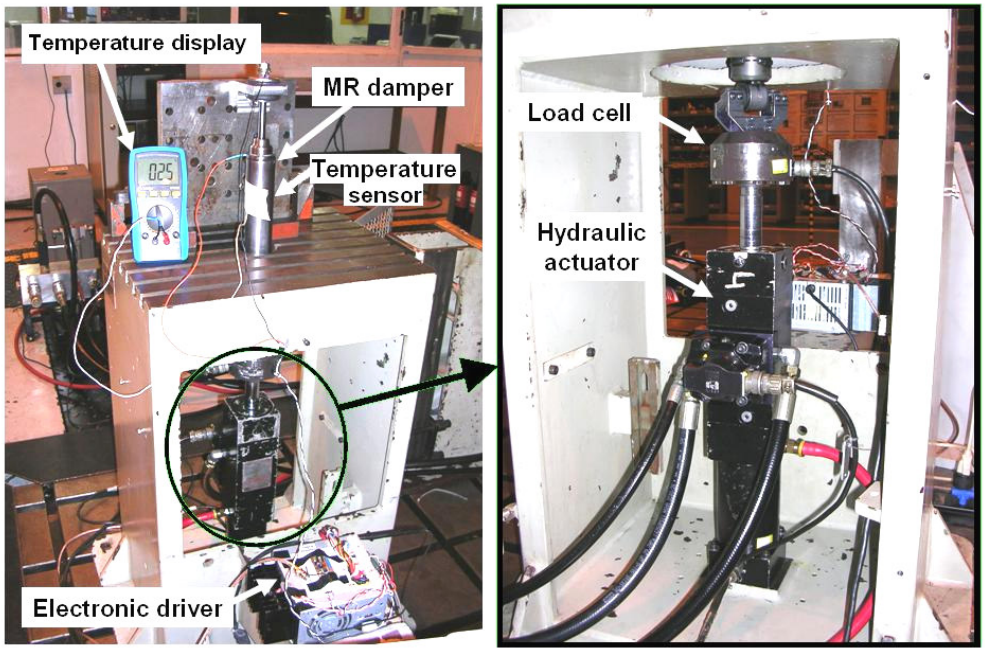

Figure 6 – Physical implementation of MR Damper test.

A temperature sensor was used to measure the temperature over the surface of damper. Experimental data were taken only when this temperature was around 60 ºC (±5 ºC). This care is necessary since 60 ºC is the operational work temperature of the damper, and the MR fluid has a high viscosity at 25 ºC. On the other hand, for temperatures over 60 ºC, there are only little changes in MR fluid behavior, which can be disregarded.

The MTS FlexTest GT was the equipment used to generate and to monitor the signals.

6. EXPERIMENTAL DATA

Three experiments were developed to acquire the necessary data for the model identification. In the first one, it was imposed to the damper a displacement varying between ±30mm in an 1Hz sinusoidal signal. During the sinusoidal displacement it were applied steps of 2 volts in the damper control input, varying the tension between 0 and 10 volts. The force signal was measured by a load cell and recorded, as showed in Fig 8. This experiment allows getting information about the general behavior of the MR damper.

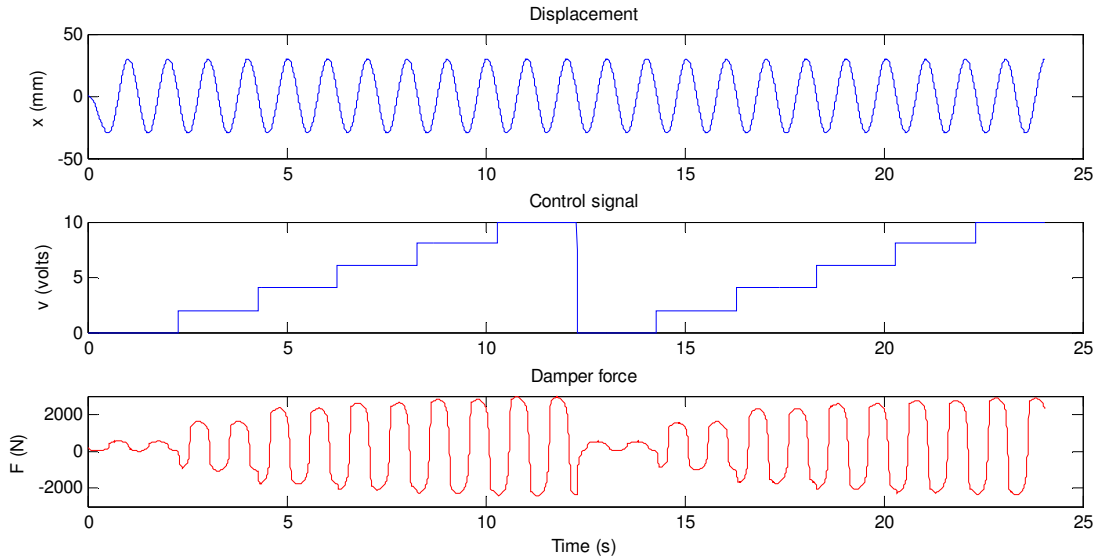

Figure 8 – First experiment data.

In the second experiment it was applied a triangular displacement with 15mm amplitude and 1Hz, and in the middle of some ramps it were applied steps from 0 to 8 volts or 8 to 0 volts, as show in Fig. 9A. The damper resultant force was also recorded. This experiment produces information for a step response behavior of the MR damper.

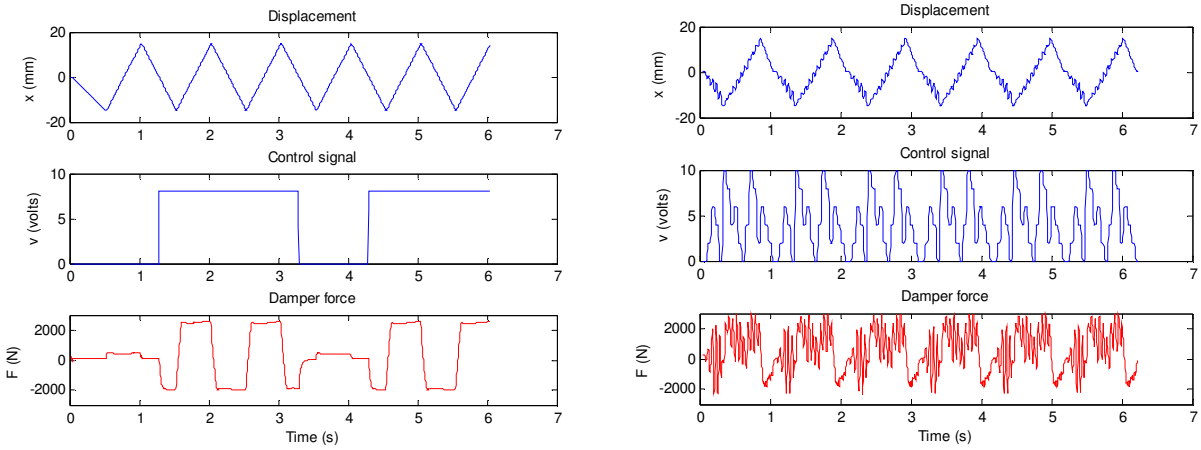

Figure 9 – Second experiment data (A) and third experiment data (B).

In the third experiment it was applied a triangular displacement with 15mm amplitude and 1Hz, added to a sinusoidal signal with 3mm amplitude, and a random tension signal was applied in the control input, as show in Fig. 9B. This experiment leads to get information focused in the behavior of the MR damper near its real condition of work.

All signals were sampled at 1024Hz, but the sample frequency was reduced by taking one sample at each four, and making the average of those four samples to reduce the noise. Therefore the sample rate resulted in h = 3.91 ms. Afterwards, the velocities signals were calculated by a numerical differentiation of the displacement signals as follows:

$$v_x(k) = \frac{x(k+1) - x(k-1)}{2h} \tag{23}$$

7. MODEL IDENTIFICATION

A constrained nonlinear optimization was used to obtain the 21 parameters of the proposed model. The optimization was performed using a sequential quadratic programming algorithm available in MATLAB™ through the function "fminimax". This Matlab function solves the following problem:

$$\underset{x}{Min}\{Max\{FUN(x)\}\} \tag{24}$$

In Eq. (23), FUN is a Matlab function especially created for this work, which solves the difference equation for the whole period of time of the sampled data and return a vector with the 1 and 2 norms of the vector of differences between the measured force and the estimated force. The model identification process consists in the parameters adjustments to minimize the cost, i.e., the norms of error vector.

Table 1 shows the initial values and the bounds of each parameter. The last two columns of table 1 are the final values of the parameters for the identified model and its respective unit.

The lower bound of k_o is negative and the upper bound of ξ is relatively high, improving the convergence of the method by the avoidance of local minima. Other presets used in fminimax function are: TolX = TolCon = TolFun =10^{-6}, MaxFunEvas = 3000, DiffMaxChange = 10^{-3}, DiffMinChange = 10^{-8}, MinAbsMax = 2.

The optimization process time is 1 min and 18s in a PC with processor Intel™ Centrino™ Duo Core™ T2300, with 1.66 GHz clock frequency, and 1Gbytes of RAM.

The model identification process was performed over all of the three experimental data in the same time aiming a model with good performance in several situations of work, which was called *generalist model*. Of course, the identification process could be applied to each experimental data separately, which would lead to a better approximation of experimental data, but the generality of the model is lost.

Table 1. Parameters of the model.

Parameter	Initial value	Lower boundary	upper boundary	Adjusted value	Unit
η	40	4	200	**38.66**	Hz
γ_a	180000	20000	1500000	**49905**	$1/m^2$
γ_b	0	-10000	10000	**-5151**	$1/m^2.V^2$
γ_c	0	-500	500	**152.1**	$1/m^2.V^3$
β_a	80000	-400000	1500000	**-8905**	$1/m^2$
β_b	0	-1000	1000	**624.2**	$1/m^2.V^2$
A_a	50	1	1000	**21.62**	–
A_b	0	-1000	1000	**-1.578**	1/V
A_c	0	-100	100	**0.0786**	$1/V^2$
ξ	1	0,9	5	**1.012**	–
α_a	3500	-10000	500000	**4755**	N/m
α_b	10000	-35000	35000	**15717**	N/m.V
α_c	3000	-1000	50000	**3695**	$N/m.V^2$
α_d	-500	-9500	9500	**-1677**	$N/m.V^3$
α_e	-100	-300	300	**200.8**	$N/m.V^4$
α_f	7	-20	20	**-7.972**	$N/m.V^5$
c_{oa}	1500	50	5000	**868.0**	N.s/m
c_{ob}	500	-1000	2000	**486.3**	N.s/m.V
c_{oc}	0	-500	500	**-37.13**	$N.s/m.V^2$
k_o	-100	-500	120	**43.26**	N/mm
x_o	10	1	30	**6.33**	mm

8. RESULTS AND ANALYSIS

On the next graphics (Fig. 10, 11 and 12), it is shown the generalist model performance for each experimental data separately.

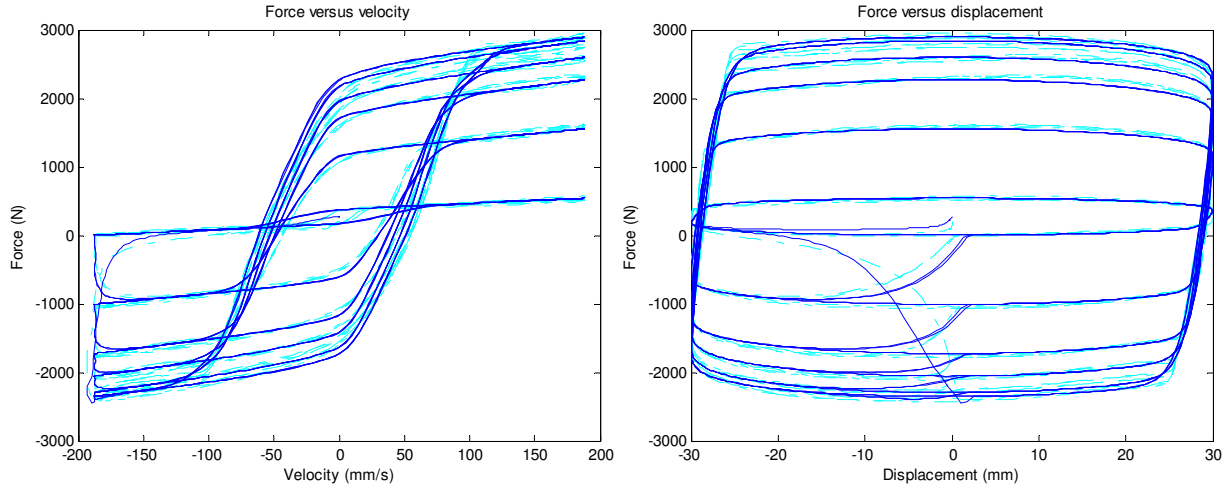

Figure 10 – Comparison between first experiment and model simulation. The darker continuous line is the model simulation result.

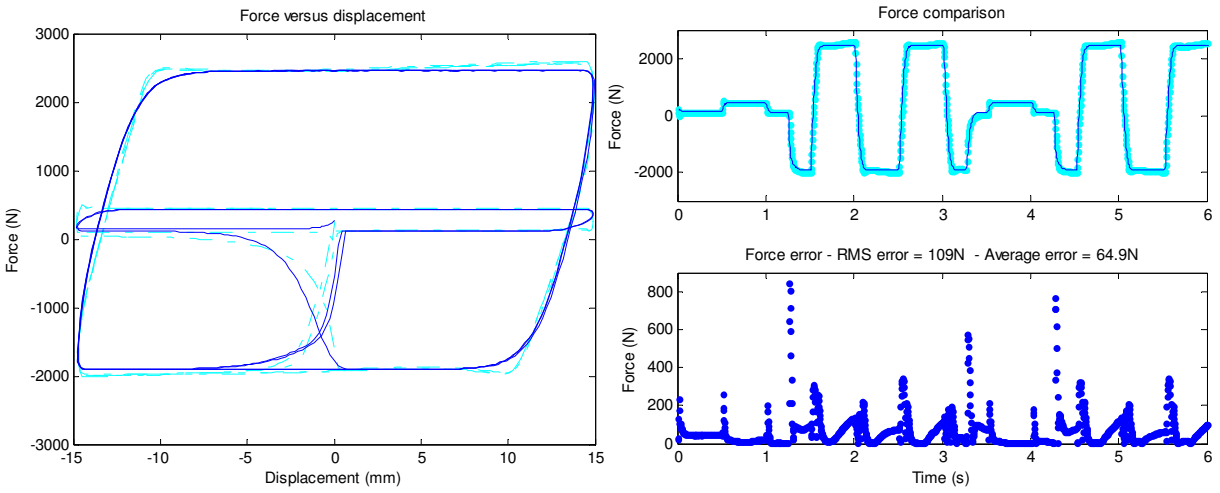

Figure 11 – Comparison between second experiment and model simulation. The darker continuous line is the model simulation result.

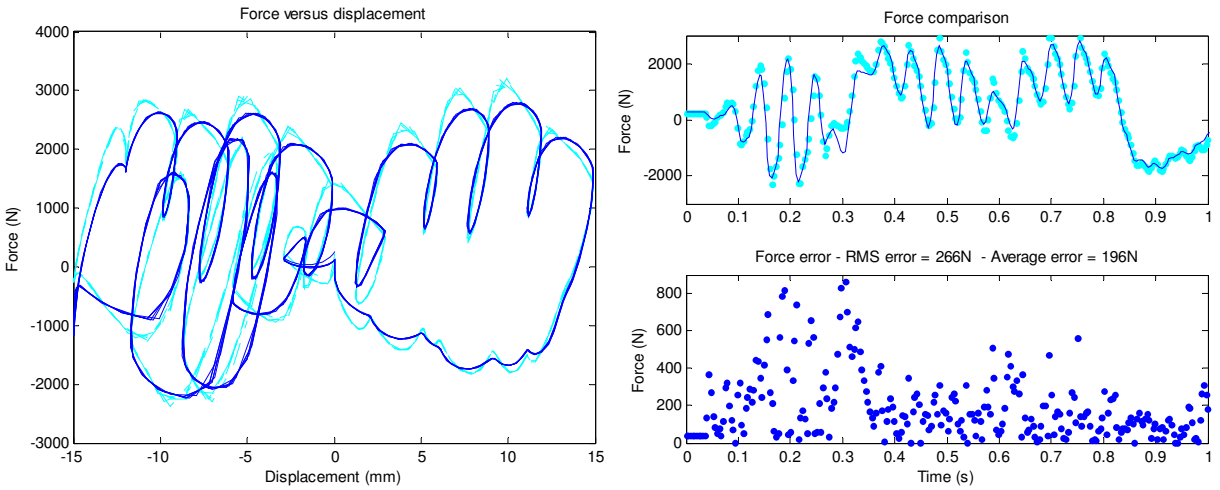

Figure 12 – Comparison between third experiment and model simulation. The darker continuous line is the model simulation result.

As shown by the graphics of experimental data and model simulation results, the proposed model effectively fits the real behavior of MR damper tested. Although the peaks of error could reach 900N, they occur in a brief period of time and do not impair significantly the general performance of the model, which presents only 266N of root-mean-square error (RMSE) in the worst case, which is less than 10% of the maximum force of the actuator.

9. CONCLUSION

The MR damper is an attractive semi-active control device that appears to have significant potential for structural and automotive control applications. To take full advantage of the unique features of the MR dampers, a high fidelity model is needed for control design and analysis.

The main goal of this work was to develop a discrete-time model for MR dampers to be used in digital implementations of control applications. In a review of several idealized mechanical models for controllable fluid dampers, a Bouc-Wen model from Spencer *et al.* (1996) was chosen to be the base of discrete-time model. The Bouc-Wen model is especially good because it is numerically tractable and is capable of exhibiting a wide variety of hysteretic behaviors. Subsequently a new discrete-time model has been proposed using a discrete-time representation of Bouc-Wen hysteresis model, which was develop by using the backward-difference approximation to map the continuous-time system into a stable discrete system. To obtain a model that reproduces the behavior of the damper

with fluctuating magnetic field, five parameters are assumed to vary with the applied voltage. Additionally, as the original continuous-time model, a time-discrete form of a first order filter has been incorporated into the model to account for the dynamics involved in the MR fluid reaching rheological equilibrium. When compared with experimental data, the resulting model was shown to accurately predict the response of the MR damper over a wide range of operating conditions, including step voltage and a multi-periodic displacement combined with random voltage tests. These results indicate that the proposed model can be effectively used for digital control algorithm development and system evaluation.

Although the proposed model has a large amount of parameters, it converges more quickly and smoothly to the experimental data, as observed during this work development, than the equivalent continuous-time model with eleven parameters, which means that the proposed model is more practical and efficient to be used in semi-active control applications development.

10. ACKNOWLEDGEMENTS

The authors would like to express their appreciation to Prof. Dr. Antônio Bombard from UNIFEI, MG, who provided the MR fluid for our experimental tests; to the Dana Nakata test laboratory team, who was very collaborative and creative in the experimental activities; to Affinia Automotive Group, in name of Eng. Eduardo Alves and Eng. Hideo Matsuzaki, due to the build of some prototype parts; and to other Dana Brazil employees that directly or indirectly participate in this project.

11. REFERENCES

Bodie, M. O.; Hać, A.; 2000, "Closed Loop Yaw Control of Vehicles Using Magneto-Rheological Dampers**".** SAE 2000 World Congress, 2000-01-0107, Detroit, Michigan, March 6-9.

Bombard, A. J. F.; Knobel, M.; Alcântara, M. R.; Joekes, I.; 2002, "Evaluation of Magnetorheological Suspensions Based on Carbonil Iron Powders". Journal of Intelligent Material Systems and Structures, Vol. 3, jul-ago.

Bombard, A. J. F.; 2005, "Suspensões Magneto-Reológicas de Pós de Ferro Carbonilo: Um Estudo da Influência das Propriedades Magnéticas e do Tamanho das Partículas". 144p. Tese (Doutorado) – Instituto de Química da Universidade Estadual de Campinas, UNICAMP. Campinas - SP.

Breese, D. G.; Gordaninejad, F.; 2003, "Semi-Active, Fail-Safe Magneto-Rheological Fluid Dampers for Mountain Bicycles**"**. International J. Vehicle Design, in press.

Carlson, J. D.; Catanzarite, D. M.; Clair, K. A.St.; 1999, "Commercial Magneto-rheological Fluid Devices**"**. Lord Corporation, Cary, NC.

Chrzan, M.J.; Carlson, J. D., 2001, "MR Fluid Sponge Devices and Their Use in Vibration Control of Washing Machines". Proceedings of the 8th Annual Symposium on Smart Structures and Materials, Newport Beach, CA.

Crivellaro, C., Tamai, E., 2003, "Study of Ride and Handling Improvement of a Pickup Light Truck Using Robust Semi-ative Suspesion Control based on Magneto-rheological Dampers". Cobem 2003 – 17th International Congress of Mechanical Engineering, #1399, São Paulo, Nov. 10-14.

Crivellaro, C.; Santos, E. C. A. dos; 2004, "Projeto de um Amortecedor Magneto-reológico". SAEBrasil 2004 International Congress, 2004-01-3279, São Paulo, SP, Brazil, November.

Dyke, S. J.; Spencer Jr., B. F.; Sain, M. K.; Carlson, J.D, 1996, "Seismic Response Reduction Using Magneto-rheological Dampers". Proceedings of the IFAC World Congress, San Francisco, California, June 30 – July 5.

Gilbert, R.; Jackson, M.; 2002, "Magnetic Ride Control" GM Tech Link, GM Dealership Service Professionals, Jan., v.4, n.1.

Hać, A.; Youn, I.; Chen, H. H., 1996, "Control of Suspensions for Vehicles With Flexible Bodies - Part II: Semi-active Suspensions". Transactions of the ASME, v.118, Sept., pp. 518-525.

Medical Product Manufacturing News, 2000, "State-of-the-Art Prosthetic Leg Incorporates Magneto-Rheological Technology". Originally Published November 2000; MPMN, 11444 W. Olympic Blvd., Los Angeles, CA 90064-1549, 310, pp. 445-426.

Ni, Y. Q.; Ko, J. M.; Chen, Z. Q.; Wang, X. Y.; Spencer, B. F., 2002, "Implementation of smart MR dampers to Dongting Lake Bridge for mitigating rain-wind-induced cable vibration". Department of Civil and Structural Engineering, The Hong Kong Polytechnic University - Hung Hom, Kowloon, Hong Kong.

Spencer, B. F., Jr.; Dyke, S. J.; Sain, M. K.; Carlson, J. D.; 1996, "Phenomenological Model of a Magneto-rheological Damper". ASCE Journal of Engineering Mechanics – March 10th.

12. RESPONSIBILITY NOTICE

The authors are the only responsible for the printed material included in this paper.